THE JOURNAL OF BIOLOGICAL CHEMISTRY
Vol. 278, No. 33, Issue of August 15, pp. 31290–31296, 2003
Printed in U.S.A.

An Electrical Potential in the Access Channel of Catalases Enhances Catalysis*

Received for publication, April 17, 2003, and in revised form, May 29, 2003
Published, JBC Papers in Press, May 29, 2003, DOI 10.1074/jbc.M304076200

Prashen Chelikani‡, Xavi Carpena§, Ignacio Fita§, and Peter C. Loewen‡¶

From the ‡Department of Microbiology, University of Manitoba, Winnipeg, Manitoba R3T 2N2, Canada and the §Institut de Biología Molecular de Barcelona, Consejo Superior de Investigaciones Cientificas, Jordi-Girona 18-26, 08034 Barcelona, Spain

Substrate H_2O_2 must gain access to the deeply buried active site of catalases through channels of 30–50 Å in length. The most prominent or main channel approaches the active site perpendicular to the plane of the heme and contains a number of residues that are conserved in all catalases. Changes in Val^{169}, 8 Å from the heme in catalase HPII from *Escherichia coli*, introducing smaller, larger or polar side chains reduces the catalase activity. Changes in Asp^{181}, 12 Å from the heme, reduces activity by up to 90% if the negatively charged side chain is removed when Ala, Gln, Ser, Asn, or Ile are the substituted residues. Only the D181E variant retains wild type activity. Determination of the crystal structures of the Glu^{181}, Ala^{181}, Ser^{181}, and Gln^{181} variants of HPII reveals lower water occupancy in the main channel of the less active variants, particularly at the position forming the sixth ligand to the heme iron and in the hydrophobic, constricted region adjacent to Val^{169}. It is proposed that an electrical potential exists between the negatively charged aspartate (or glutamate) side chain at position 181 and the positively charged heme iron 12 Å distant. The potential field acts upon the electrical dipoles of water generating a common orientation that favors hydrogen bond formation and promotes interaction with the heme iron. Substrate hydrogen peroxide would be affected similarly and would enter the active site oriented optimally for interaction with active site residues.

The monofunctional catalase (hydrogen peroxide:hydrogen peroxide oxidoreductase, EC 1.11.1.6) is a protective enzyme that degrades hydrogen peroxide to prevent damage from it or its more reactive degradation byproducts. The catalase reaction utilizes hydrogen peroxide as both an electron donor and an electron acceptor as summarized in the overall Reaction 1, which involves two distinct stages. In the first stage (Reaction 2) the resting state enzyme is oxidized by hydrogen peroxide to an oxy-ferryl intermediate, compound I, which in the second stage (Reaction 3) is reduced back to the resting state by a second hydrogen peroxide.

$$2H_2O_2 \rightarrow 2H_2O + O_2$$

$$\text{Enz (Por-Fe}^{III}\text{)} + H_2O_2 \rightarrow \text{Cpd I (Por}^{+\cdot} - \text{Fe}^{IV} = O) + H_2O$$

$$\text{Cpd I (Por}^{+\cdot} - \text{Fe}^{IV} = O) + H_2O_2 \rightarrow \text{Enz (Por} - \text{Fe}^{III}) + H_2O + O_2$$

REACTIONS 1–3

The structures of heme-containing monofunctional catalases isolated from eight different sources have been reported including those from bovine liver (1, 2), human erythrocytes (3, 4), *Penicillium vitale* (5, 6), *Saccharomyces cerevisiae* (7), *Proteus mirabilis* (8), *Micrococcus lysodeikticus* (9), *Escherichia coli* (10, 11), and *Pseudomonas syringae* (12), revealing a highly conserved β-barrel core structure in all enzymes. The active center, composed of a heme with a tyrosine as the fifth ligand to the iron, a histidine, and an asparagine, is deeply buried in this core structure. HPII from *E. coli* contains two post-translational modifications in the active center, including an oxidized, *cis*-spirolactone, heme d (13), and a covalent bond between the N^{δ} of His^{392} and the C^{β} of Tyr^{415}, the proximal side fifth ligand of the heme (14). Both modifications are generated self-catalytically by the catalase and seem to require some degree of catalase activity (15). Three channels, the main channel oriented perpendicular to the plane of the heme, the lateral channel approaching in the plane of the heme, and a channel leading to the central cavity, connect the active site to the exterior of the enzyme, providing routes for substrate ingress and product egress.

A number of catalase HPII variants have been constructed (16) to study the roles of various residues in the enzyme, including the active site residues. Most recently, the characterization of inactive variants has allowed the identification of substrate H_2O_2 localized in the main or perpendicular channel (17). The presence of H_2O_2 in the channel of HPII, the relatively direct route provided by the main channel to the heme in other catalases, and molecular dynamic studies (18, 19) all suggest that the main channel is the primary route for substrate movement to the active site. On the other hand, evidence has been presented that the lateral channel in HPII does have a role (20).

A number of highly conserved residues are situated in the main channel. These include the essential histidine, a valine and an aspartate, (His^{128}, Val^{169}, and Asp^{181} in HPII) situated 4, 8, and 12 Å from the heme, respectively (Fig. 1). His^{128} is essential for catalysis in HPII (15), and the importance of Val^{169} in constricting the narrowest, hydrophobic portion of the channel has been investigated in yeast CATA (7) and HPII (21), although without a definitive conclusion. The importance of the other residues further up the channel has not been studied, and this paper focuses on a number of these residues in the main

* This work was supported by Grant BIO2002-04419 from Direccion General de Investigacion Ciencia y Technologia (to I. F.) and Grant OGP9600 from the Natural Sciences and Engineering Research Council of Canada (to P. C. L.). The costs of publication of this article were defrayed in part by the payment of page charges. This article must therefore be hereby marked "*advertisement*" in accordance with 18 U.S.C. Section 1734 solely to indicate this fact.

The atomic coordinates and structure factors (code 1P7Y, 1P7Z, 1P80, and 1P81) have been deposited in the Protein Data Bank, Research Collaboratory for Structural Bioinformatics, Rutgers University, New Brunswick, NJ (http://www.rcsb.org/).

¶ To whom correspondence should be addressed: Dept. of Microbiology, University of Manitoba, Winnipeg, MB R3T 2N2, Canada. Tel.: 204-474-8334; Fax: 204-474-7603; E-mail: peter_loewen@umanitoba.ca.

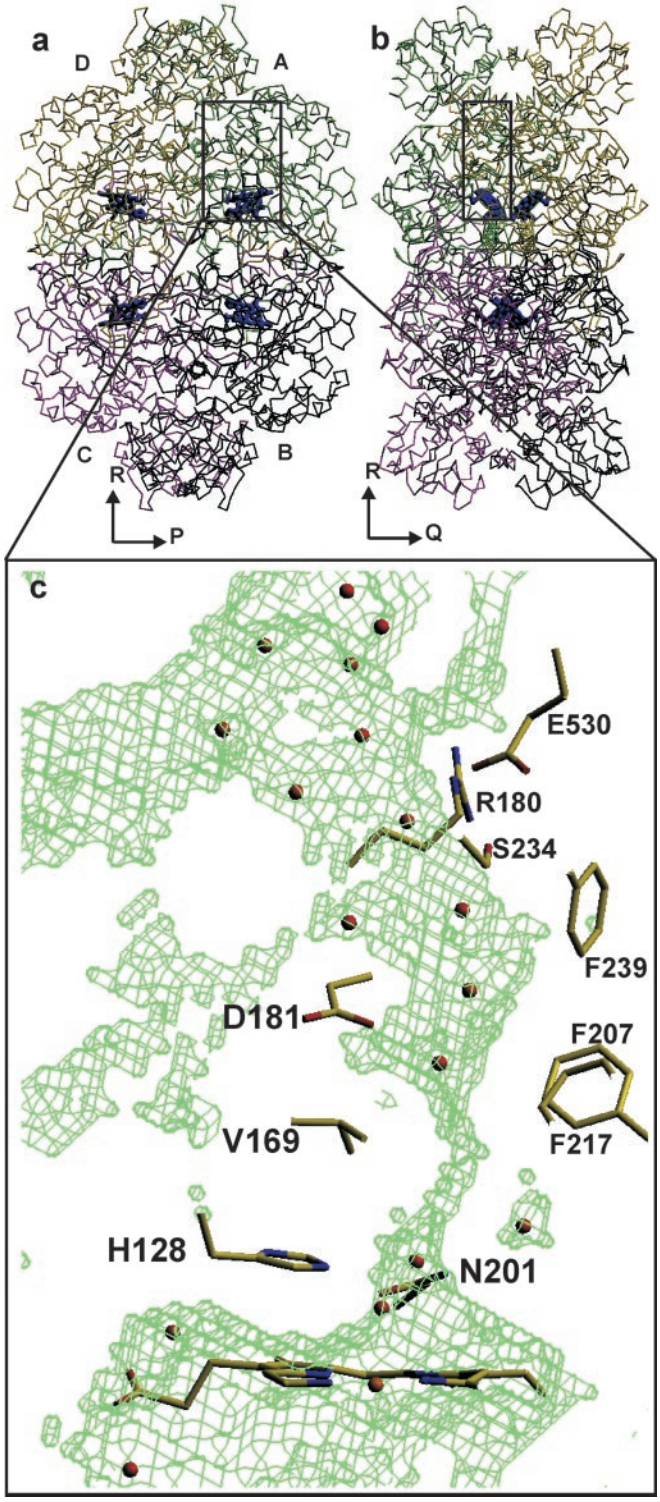

FIG. 1. **Location of the main channel accessing the active sites of HPII.** The images of HPII in *a* and *b* are rotated 90° relative to each other as indicated by the associated axes to clearly demonstrate the deeply buried location of the heme active site. Subunits A (*green*), B (*blue*), C (*red*), and D (*gold*) are also indicated in *a*. The portion of subunit A where the channel is located is indicated by the *box* in *a*, and this section is enlarged in *c*. In *c*, a slab of the protein is presented showing the lower 30 Å of the channel after two branches merge. The program VOIDOO depicts the surface of the channel as a *green wire mesh*. The locations of the key residues His[128], Asn[201], Val[169], and Asp[181] are indicated. Residues further up the channel, Arg[180], Ser[234], and Glu[530] are also indicated for reference. Residues Phe[207], Phe[217], and Phe[239] adjacent to Val[169] are included to illustrate the hydrophobic, constricted nature of the channel. The locations of the ordered water molecules in the native structure are indicated by *red spheres*.

TABLE I
Oligonucleotides and katE restriction fragments used in oligonucleotide-directed mutagenesis of katE

Mutant	Sequence change	Oligonucleotide[a]	Restriction fragment
V169I	(GTT → ATT)	TTCTCTACC**ATT**CAGGGTGGT	*Hin*dIII-*Eco*RI (1246–1856)
V169F	(GTT → TTT)	TTCTCTACC**TTT**CAGGGTGGT	*Hin*dIII-*Eco*RI (1246–1856)
V169W	(GTT → TGG)	TTCTCTACC**TGG**CAGGGTGGT	*Hin*dIII-*Eco*RI (1246–1856)
R180A	(CGT → GCT)	GATACCGTG**GCT**GATATCCGT	*Hin*dIII-*Eco*RI (1246–1856)
R180K	(CGT → AAA)	GATACCGTG**AAA**GATATCCGT	*Hin*dIII-*Eco*RI (1246–1856)
D181A	(GAT → GCT)	ACCGTGCGT**GCT**ATCCGTGGC	*Hin*dIII-*Eco*RI (1246–1856)
D181S	(GAT → TCT)	ACCGTGCGT**TCT**ATCCGTGGC	*Hin*dIII-*Eco*RI (1246–1856)
D181E	(GAT → GAA)	ACCGTGCGT**GAA**ATCCGTGGC	*Hin*dIII-*Eco*RI (1246–1856)
D181Q	(GAT → CAA)	ACCGTGCGT**CAA**ATCCGTGGC	*Hin*dIII-*Eco*RI (1246–1856)
D181N	(GAT → AAT)	ACCGTGCGT**AAT**ATCCGTGGC	*Hin*dIII-*Eco*RI (1246–1856)
D181I	(GAT → ATT)	ACCGTGCGT**ATT**ATCCGTGGC	*Hin*dIII-*Eco*RI (1246–1856)
D181W	(GAT → TGG)	ACCGTGCGT**TGG**ATCCGTGGC	*Hin*dIII-*Eco*RI (1246–1856)

[a] The sequence in bold type is the codon that has been modified.

TABLE II
Specific activity of purified catalase variants and heme composition

Variant	Specific activity	Heme
	units/mg	
Wild type	19,100 ± 900	d
V169I	3,730 ± 400	d
V169F	1,470 ± 120	d
V169W	ND[a]	
R180A	11,200 ± 1,510	d
R180K	22,700 ± 1,650	d
D181A	810 ± 60	b
D181S	2,550 ± 190	b
D181E	21,900 ± 700	d
D181Q	1,770 ± 50	b
D181N	2,800 ± 400	b
D181I	2,330 ± 350	b
D181W	ND	

[a] ND, not determined because no protein accumulated.

channel of HPII. The importance of the highly conserved aspartate, Asp[181], in particular the negative charge on its side chain, is revealed.

EXPERIMENTAL PROCEDURES

Materials—Standard chemicals and biochemicals were obtained from Sigma. Restriction nucleases, polynucleotide kinase, DNA ligase, and the Klenow fragment of DNA polymerase were obtained from Invitrogen.

Strains and Plasmids—The plasmid pAMkatE72 (22) was used as the source for the *katE* gene. Phagemids pKS+ and pKS− from Stratagene Cloning Systems were used for mutagenesis, sequencing, and cloning. *E. coli* strains NM522 (*supE thi* (*lac-proAB*) *hsd-5* [F′ *proAB lacI*^{q} *lacZ*)*15*]) (23), JM109 (*recA1 supE44 endA1 hsdR17 gyrA96 relA1 thi*) (*lac-proAB*) (24), and CJ236 (*dut-1 ung-1 thi-1 relA1*/pCJ105 F′) (25) were used as hosts for the plasmids and for generation of single-strand phage DNA using helper phage R408. Strain UM255 (*pro leu rpsL hsdM hsdR endI lacY katG2 katE12*::Tn10 *recA* (26) was used for expression of the mutant *katE* constructs and isolation of the mutant HPII proteins.

Oligonucleotide-directed Mutagenesis—Oligonucleotides were purchased from Invitrogen and are listed in Table I. The restriction nuclease fragments that were mutagenized following the Kunkel procedure (25), sequenced, and subsequently reincorporated into pAMkatE72 to generate the plasmids encoding the mutagenized *katE* genes are also listed. Sequence confirmation of all sequences was by the Sanger

TABLE III
Data collection and structural refinement statistics for the Asp[181] variants of HPII

	D181A	D181S	D181Q	D181E
Data collection statistics				
Space group	$P2_1$	$P2_1$	$P2_1$	$P2_1$
Cell				
a (Å)	93.11	93.34	93.76	93.38
b (Å)	132.50	132.88	133.13	132.86
c (Å)	121.49	121.45	122.50	122.04
β^0	109.5	109.4	109.5	109.5
Resolution range (Å)	29.8-2.4 (2.49-2.4)[a]	29.8-2.2 (2.27-2.2)	29.8-1.65 (1.71-1.65)	29.9-1.8 (1.86-1.8)
Unique reflections ($F > 0$)	105,578 (7,994)	138,759 (11,109)	323,591 (23,749)	251,911 (20,645)
Completeness (%)	96.8 (88.8)	99.6 (99.5)	96.0 (79.4)	99.2 (98.0)
$I/\sigma(I)$	9.8	8.5	10.6	7.5
R_{sym} (%)[b]	13.5	10.0	10.7	9.6
Refinement statistics				
Working set	100,246 (7,579)	131,677 (10,519)	307,191 (22,578)	239,324 (19,579)
Free reflections	5,332 (415)	6,965 (590)	16,400 (1,171)	12,587 (1,066)
R_{cryst} (%)[c]	14.4 (18.7)	15.2 (17.4)	17.4 (23.3)	17.7 (23.2)
R_{free} (%)	22.5 (27.8)	21.6 (25.2)	20.6 (26.7)	21.8 (26.5)
No. of non-hydrogen atoms				
Protein	22,972	22,976	22,988	22,988
Water	2,767	2,733	3,221	3,072
Heme	172	172	172	176
Root mean square deviation from ideality				
Bond lengths (Å)	0.012	0.012	0.008	0.011
Bond angles (deg.)	2.4	2.0	1.6	1.6
Peptide planarity (Å)	0.024	0.023	0.020	0.022
Aromatic planarity (Å)	0.012	0.012	0.007	0.010
Est. coordinate error (Luzzati) (Å)	0.20	0.18	0.17	0.18
Averaged B factor (Å^2)				
Main chain	26.2	22.2	18.2	16.3
Side chain	26.2	22.7	19.5	17.1
Water	31.9	29.6	31.2	26.

[a] Values in parentheses correspond to the highest resolution shell.
[b] $R_{sym} = \Sigma_{hkl}\,\Sigma_j|I_{hklj} - \langle I_{hkl}\rangle|/\Sigma_{hkl}\langle I_{hkl}\rangle$.
[c] $R_{cryst} = \Sigma||F_{obs}| - |F_{calc}||/\Sigma|F_{obs}|$. R_{free} is as for R_{cryst} but calculated for a test set comprising reflections not used in the refinement (5%).

method (27) on double-stranded plasmid DNA generated in JM109. Subsequent expression and purification were carried out as described previously (15).

Catalase, Protein, and Spectral Determination—Catalase activity was determined by the method of Rorth and Jensen (28) in a Gilson oxygraph equipped with a Clark electrode. One unit of catalase is defined as the amount that decomposes 1 μmol of H_2O_2 in 1 min in a 60 mM H_2O_2 solution at pH 7.0 at 37 °C. The initial rates of oxygen evolution were used to determine the turnover rates to minimize the inactivation caused by high [H_2O_2] (29). Protein was estimated according to the methods outlined by Layne (30). The absorption spectra were obtained using a Milton Roy MR3000 spectrophotometer. The samples were dissolved in 50 mM potassium phosphate, pH 7.0.

Enzyme Purification—Cultures of *E. coli* strain UM255 transformed with plasmids pAMkatE72, pD181A, pD181S, pD181Q, pD181N, and pD181E, encoding HPII or the Ala[181], Ser[181], Gln[181], Asn[181], and Glu[181] variants, respectively, were grown in Luria broth containing 10 g/liter tryptone, 5 g/liter yeast extract, and 5 g/liter NaCl. Growth of the mutant variants was for 16 h at 37 °C or 22 h at 28 °C and of the wild type HPII was for 16 h at 37 °C with shaking. The cells were harvested, and HPII was isolated as previously described (31). Following resuspension of the ammonium sulfate fraction, the solution was heated at 50 °C for 15 min followed by centrifugation prior to chromatography on DEAE cellulose (Whatman).

Crystallization, Data Collection, and Refinement—Crystals of the Asp[181] variants of HPII were obtained at 22 °C using the hanging drop vapor diffusion method over a reservoir solution containing 15–17% PEG 3350 (Carbowax), 1.6–1.7 M LiCl (Baker), and 0.1 M Tris, pH 9.0. The crystals were monoclinic, space group $P2_1$ with one tetrameric molecule in the crystal asymmetric unit and had a solvent content of ~40%. The diffraction data were obtained from crystals transferred to a solution containing 30% PEG 3350 and flash cooled with a nitrogen cryo-stream giving unit cell parameters listed in Table III. The diffraction data were autoindexed and integrated using programs DENZO and merged using SCALEPACK (32) (see Table III).

Structure determination was carried out with the program MOLREP using native HPII as the initial searching model. Refinements were completed using the program REFMAC (33) with solvent molecules modeled with the program WATPEAK (34) and manually with the graphics program O (35). Solvent molecules were only introduced when they corresponded to the strongest peaks in the difference Fourier maps that could make at least one hydrogen bond with atoms already in the model. In the final rounds of refinement the four subunits were treated independently with the bulk solvent correction applied and the whole resolution range available used for each variant. The analysis of solvent accessibility and molecular cavities was carried out with program VOIDOO (36) using a reduced atomic radius for polar atoms in accounting for possible hydrogen bonds (21). All of the figures were prepared using SETOR (37). The structure factors and coordinates have been submitted to the Protein Data Bank under the accession numbers 1P7Y for D181A, 1P7Z for D181S, 1P80 for D181Q, and 1P81 for D181E.

RESULTS

Effect of Changes in Val[169] Situated 8 Å from the Heme—A conserved valine is situated in the main channel of all catalases approximately 8 Å from heme. Its side chain causes a constriction or narrowing of the channel to a diameter of approximately 3 Å that prevents any molecules much larger than H_2O and H_2O_2 from gaining access to the active site heme. Changing this valine to alanine in yeast catalase CATA (7) allowed an increase in peroxidatic activity consistent with the concept that valine restricted access of larger molecules to the active site. Counterintuitively, the valine to alanine change in both CATA and HPII also caused a decrease in catalase activity, leading to the conclusion that the dimensions or volume of the channel were critical in determining the rate of H_2O_2 movement into the active site. Introducing the possibility for hydrogen bonding between water and protein in the V169S variant (12) also decreased the efficiency of the catalase reaction. To expand the study of Val[169], the effect of larger side chains at this location in HPII was investigated with the construction of the V169I, V169F, and V169W variants. Purification and characterization of variants V169I and V169F revealed activities that are 10–15% of wild type (Table II), even lower than those of the V169A and V169S, consistent with the larger side chains interfering with substrate access to the active site. Heme conversion from

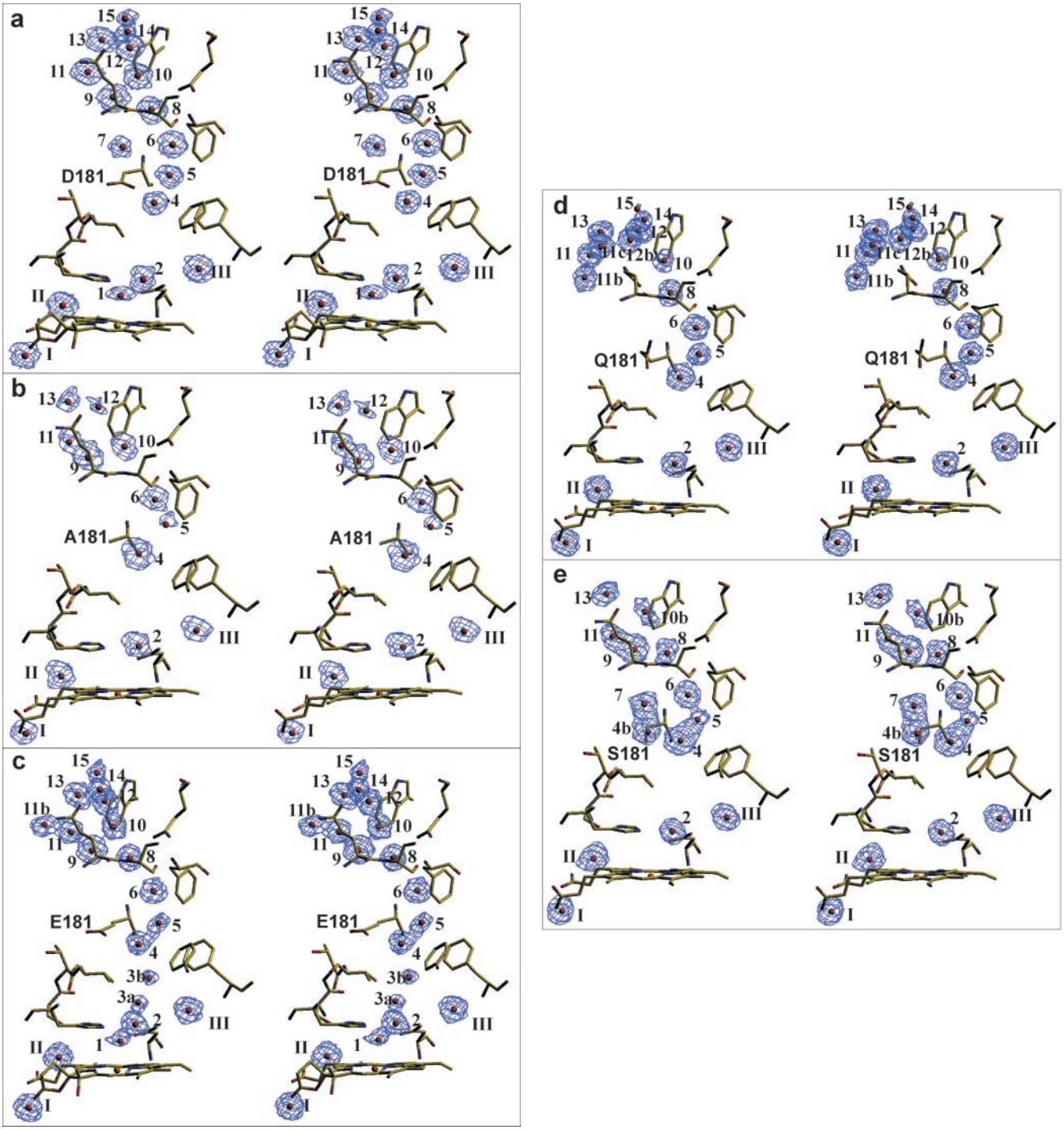

FIG. 2. **Stereo diagrams of the water distribution in the main channel of native HPII (*a*), the D181A variant (*b*), the D181E variant (*c*), the D181Q variant (*d*), and the D181S variant (*e*).** The $2F_o - F_c$ electron density corresponding to the individual water molecules is modeled at 1 σ and shown as a *blue wire mesh*. The map for native HPII was derived from Protein Data Bank submission 1GGE and its associated structure factors. The numbering scheme for the waters is the same as in Table IV where the occupancy or B factors for the various waters are listed.

heme b to heme d was normal despite the lower catalytic rate. The V169W variant did not accumulate protein, presumably because protein folding was adversely affected by the larger side chain, and the nascent protein was proteolyzed.

Effect of Changes to Asp^{181} Situated 12 Å from the Heme—A conserved aspartate is present in the main channel of all catalases approximately 12 Å from the heme. The role of this residue has not been investigated in any catalase, and *katE* was mutated to express the HPII variants D181A, D181S, D181Q, D181N, D181I, D181E, and D181W (Table I). Purified variants D181A, D181S, D181Q, D181N, and D181I all exhibited between 5 and 15% of wild type activity, indicating that the loss of activity was independent of side chain size or ability to form hydrogen bonds with adjacent waters. Significantly, the D181E variant retained wild type levels of activity, revealing that the presence of a negatively charged side chain at this location is critical for the catalytic process. As with the V169W variant, the D181W variant did not accumulate protein, presumably because the large side chain interfered with folding.

The crystal structures of D181A, D181S, D181Q, and D181E

TABLE IV
Water occupancy in the main or perpendicular channel of catalase HPII subunits listed as B factors (Å²)

The positions associated with the water numbering are shown in Fig. 2.

Water #	Subunit A	Subunit B	Subunit C	Subunit D
HPII (1.9 Å; 1GGE) average *B* factor: 9.2 (protein), 17.7 (water)				
1	40.0	28.1	42.7	
2	15.3	17.4	16.3	12.9
3b			32.3	
4	24.0	20.5	22.5	29.9
5	30.7	41.2	29.0	27.9
6	10.7	11.6	14.8	10.4
7	28.0	31.1	33.3	24.1
8	7.7	10.9	18.6	6.6
9	7.1	9.4	12.0	4.7
10	15.3	17.1	14.8	13.4
11	16.7	18.8	23.7	10.9
12	8.8	19.5	14.8	13.8
13	19.3	35.5		17.5
14	33.6	31.3		25.3
15	30.1		30.1	
I	3.7	7.1	4.8	6.2
II	5.1	6.1	5.0	7.1
III	4.0	8.9	6.4	8.1
D181A (2.4 Å) average *B* factor: 26.2 (protein), 31.9 (water)				
2	16.7	20.0	22.1	21.6
4	6.1	8.1	15.1	11.5
5	44.1	28.8	31.3	31.4
6	25.4	34.3	28.0	32.5
9	21.8	18.5	25.4	20.0
10	37.0	25.0	22.4	39.0
11	43.0			
12	48.9	34.1	33.4	35.0
13	39.9	45.8	47.8	44.3
15			38.0	
I	19.3	21.2	13.3	13.5
II	17.8	19.9	18.8	12.2
III	15.5	15.5	17.1	17.2
D181E (1.8 Å) average *B* factor: 16.7 (protein), 26.2 (water)				
1	35.1	43.4	44.2	46.1
2	26.5	24.9	28.4	29.4
3a	44.6	69.6	39.5	43.7
3b	34.0	30.2	32.1	25.4
4	35.0	47.5	42.3	41.7
5	37.8	36.7	37.7	32.7
6	16.0	17.0	20.1	16.5
8	20.7	22.8	37.3	17.4
9	12.6	15.8	18.1	14.9
10	26.6	33.6	28.9	24.1
11	24.8	28.2	33.7	20.4
11b	30.1	35.8		
12	19.2	20.9	21.3	23.7
13	27.5			30.9
14	36.2	37.4	48.9	28.4
15	34.4		48.9	
I	10.4	10.3	9.7	14.1
II	9.0	11.5	14.0	7.9
III	11.7	13.6	10.7	13.3
D181Q (1.65 Å) average *B* factor: 18.8 (protein), 31.2 (water)				
2	14.1	17.9	18.1	14.6
4	18.0	20.9	24.4	20.6
5	22.8	27.4	27.0	24.9
6	18.1	21.2	18.9	18.2
8	23.5	24.3	27.4	22.3
10	37.1	35.3	39.1	39.6
11	19.4	22.4	21.4	18.7
11b	23.0		23.4	22.9
11c	22.9	21.8	25.1	20.2
12	19.6	25.9	24.0	24.5
12b	30.3	22.9	27.4	31.2
13	25.9	26.8	23.5	26.6
14	34.4		31.6	
15	56.2		38.6	
I	13.5	15.3	12.9	11.9
II	11.3	11.5	14.2	13.7
II	14.3	14.2	14.6	13.2
D181S (2.2 Å) average *B* factor: 22.5 (protein), 29.6 (water)				
2	22.9	18.8	20.6	16.0
4	13.9	14.2	21.3	13.9
4b	25.1	23.2	26.6	25.6
5	39.0	47.5	53.9	54.9
6	25.3	27.2	33.9	19.7
8	33.2	32.2	37.0	32.1
9	16.5	13.7	16.1	
10b	44.8	40.8	38.4	
11	34.7	31.3		40.1
12			44.1	37.3
13	43.8	46.8		
14			44.1	
I	12.0	13.6	13.8	12.5
II	10.7	16.4	15.5	11.2
III	11.7	10.7	11.5	13.5

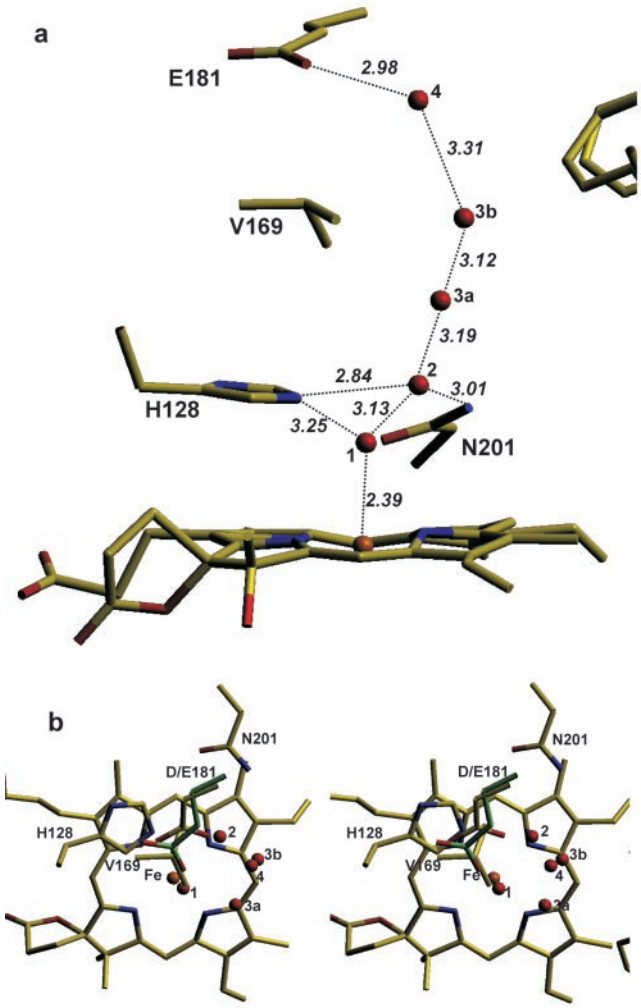

FIG. 3. *a*, schematic showing the distances among waters in the main channel of the D181E variant. The potential hydrogen bonds are shown as *dashed lines*, and the distances are expressed in Å. The water numbering is as in Fig. 2 and Table IV. *b*, stereo view oriented down the main channel toward the heme from Asp[181]. The slightly shifted location of the Glu side chain in the D181E variant is indicated in *green*. The water numbering is as in *a*.

were determined to provide insight into how Asp[181] influenced catalysis (Table III). The structures of the four variants differed from the structure of native HPII only in the immediate vicinity of the changed residue and more distantly with changes in the number and location of solvent molecules in the main channel and active site (Fig. 2). In the active site cavity, the feature common to all three inactive variants, D181A, D181S, and D181Q, is the absence of water 1, the sixth ligand of the heme, whereas nearby water 2 is present in the active sites of all variants. In addition, there are fewer waters in the channels of the less active variants generally (Table IV), even in positions over 20 Å away from the heme. By contrast, the native enzyme and the active variant D181E have water present at most positions in the channel. In particular, position 1, the sixth ligand to the heme, is occupied in three of four subunits of HPII and in all four subunits of D181E. Even the constricted, hydrophobic portion of the channel near Val[169] is occupied at 3B in one subunit of HPII and at 3A and 3B in all four subunits of D181E.

As expected there are some changes in the positions of waters in the vicinity of the modified side chain at residue 181. These changes are most extensive in the D181Q variant where the nearby Gln[233] side chain unexpectedly adopts a different

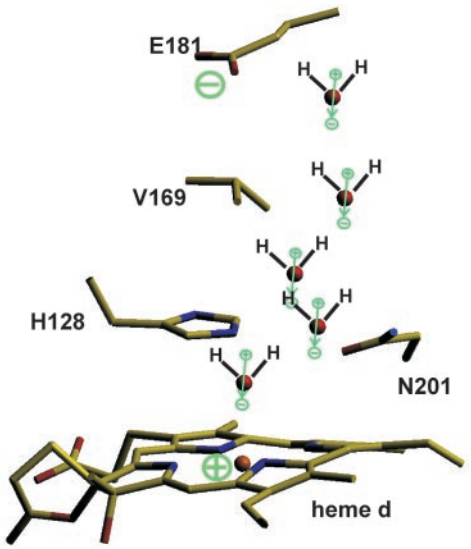

FIG. 4. **Schematic of the main channel illustrating the presence of a negative charge (in *green*) on the side chain of Glu[181] and a positive charge (in *green*) on the heme iron and the effect of the electrical potential between these two charges on the electrical dipoles of water in the channel and active site.** The orientation of the electrical dipoles is indicated by the *green arrow* over each H_2O. The location of the water molecules are those in subunit A of variant D181E.

conformation. The two waters that are adjacent to and interacting with the side chain of Asp[181] at positions 4 and 5 are present in all variants, although they are shifted approximately 0.5 Å in D181A/S/Q, indicating that the interaction with Asp[181] is not required for their presence. The three waters surrounding the heme, labeled I, II, and III, are conserved in all catalases for which structures have been determined and are included as controls.

Effect of Changes to Arg[180]—Arg[180] is a another highly conserved residue in catalases, and even though it is adjacent to Asp[181], its side chain is oriented away from the channel (Fig. 1) and is situated almost 20 Å from the heme. To determine whether the influence of residues in this region of the enzyme was general or specific, *katE* was mutated to express variants R180A and R180K. Both presented wild type activities and heme d (Table II), indicating that other residues in the vicinity of Asp[181] did not exert as great an influence on catalysis.

DISCUSSION

Even with the wealth of knowledge accumulated from over 100 years of investigation, a clear understanding of how catalase maintains high selectivity for substrate hydrogen peroxide while at the same time exhibiting turnover rates in excess of 10^6/s remains elusive. The issue of selectivity can be explained in part by the active site heme being deeply buried within the β-barrel core of the subunit, necessitating passage of the substrate through 30–50 Å of narrow channels. Such narrow channels might conceivably hinder substrate movement to the active site and creates the conceptual problem of how the product water and oxygen find their way back to the surface of the protein without interfering with substrate ingress. Molecular dynamic simulations support the concept of hydrogen peroxide entering the enzyme through the main channel but do not agree on the route of product exhaust (18, 19). Furthermore, classical molecular interaction potential calculations carried out on CATA suggest that the substrate arrives in the active site properly oriented for interaction with the heme iron and side chains of the catalytic His and Asn side chains (18).

The demonstration that a negatively charged side chain in the main channel of HPII enhances water occupancy in the access channel, particularly at the sixth ligand position and coincidently enhances enzyme activity provides a valuable insight into the mechanism of the catalase reaction. Both observations can be explained in terms of an electrical potential between the negatively charged carboxylate and the positively charged heme iron, which will influence the orientation of any molecule with an electrical dipole passing through the channel. Furthermore, given the location of the sixth ligand water in roughly the same position as substrate H_2O_2, on a direct line between the carboxylate and heme irons (Fig. 3), the electrical potential may influence transition state formation.

The hydrogens in H_2O_2 are separated by an angle of approximately 110° when viewed along the O–O axis resulting in an asymmetric or skewed structure. Orbital interactions present an energy barrier to rotation around the O–O bond of approximately 2.5 kcal/mol, limiting H_2O_2 to one predominant conformation (38). The structure gives rise to an electrical dipole of 2.3 Debye, just slightly larger than the 1.9 Debye dipole of water. Consequently, water and hydrogen peroxide passing Asp[181] in the main channel will be affected by the electrical potential and be forced into an orientation with the oxygens directed toward the heme iron (Fig. 4). When oxygen O-1 of H_2O_2 becomes associated with the heme iron, spatial constraints in the active site fix H-1 within hydrogen bond distance of the imidazole ring of the active site histidine and O-2 within hydrogen bonding distance of the NH_2 of the active site asparagine. Thus, orientation of the dipole of H_2O_2 in the potential field presents a simple mechanism to explain the prediction arising from molecular dynamic studies that substrate molecules enter the active site in a preferred orientation.

Similarly, the greater occupancy of water in the channel of the native enzyme and the D181E variant, compared with the other less active Asp[181] variants, can be attributed to the electrical potential acting on the dipoles of the solvent to create a population of waters with common orientation, thereby favoring the formation of a hydrogen bonded matrix. In the hydrophobic portion of the channel between Asp[181] and His[128], waters have only other waters to hydrogen bond with, and the bond lengths separating waters 2, 3a, 3b, and 4 are longer than optimal for strong hydrogen bonds (Fig. 3). The favorable orientation of the molecules induced by the electrical potential may be critical in stabilizing the solute matrix in the channel. What cannot be satisfactorily explained is the difference in occupancies between the channels of D181E and the native enzyme. One possibility is that it is simply an artifact of the refinement process, but the resolutions of the two data sets are approximately equivalent, and there are few other differences between the two variants. At this juncture, it seems reasonable to conclude that water occupancy in the hydrophobic portion of the channel is not a prerequisite for catalase activity, but that water can occupy the channel if certain subtle conditions, which we do not yet fully understand, are fulfilled. Certainly a complete explanation for waters in the channel and their impact on reactivity and solute selectivity involves more than simply the length of the hydrophobic region (4). At a minimum, the volume and shape of the hydrophobic region must work in concert with electrostatic influences for optimum substrate access, and electrostatic effects have an additional key role in catalysis.

REFERENCES

1. Murthy, M. R. N., Reid, T. J., Sicignano, A., Tanaka, N., and Rossmann, M. G. (1981) *J. Mol. Biol.* **152,** 465–499
2. Fita, I., Silva, A. M., Murthy, M. R. N., and Rossmann, M. G. (1986) *Acta Crystallogr. Sect. B Struct. Crystallogr. Cryst. Chem.* **42,** 497–515
3. Ko, T.-P., Safo, M. K., Musayev, F, N., Di Salvo, M. L., Wang, C., Wu, S.-H., and Abraham, D. J. (1999) *Acta Crystallogr. Sect. D Biol. Crystallogr.* **56,** 241–245

4. Putnam, C. D., Arvai, A. S., Bourne, Y., and Tainer, J. A. (1999) *J. Mol. Biol.* **296,** 295–309
5. Vainshtein, B. K., Melik-Adamyan, W. R., Barynin, V. V., Vagin, A. A., and Grebenko, A. I. (1981) *Nature* **293,** 411–412
6. Vainshtein, B. K., Melik-Adamyan, W. R., Barynin, V. V., Vagin, A. A., Grebenko, A. I., Borisov, V. V., Bartels, K. S., Fita, I., and Rossmann, M. G. (1986) *J. Mol. Biol.* **188,** 49–61
7. Maté, M. J., Zamocky, M., Nykyri, L. M., Herzog, C., Alzari, P. M., Betzel, C., Koller, F., and Fita, I. (1999) *J. Mol. Biol.* **286,** 135–139
8. Gouet, P., Jouve, H. M., and Dideberg, O. (1995) *J. Mol. Biol.* **249,** 933–954
9. Murshudov, G. N., Melik-Adamyan, W. R., Grebenko, A. I., Barynin, V. V., Vagin, A. A., Vainshtein, B. K., Dauter, Z., and Wilson, K. (1982) *FEBS Lett.* **312,** 127–131
10. Bravo, J., Verdaguer, N., Tormo, J., Betzel, C., Switala, J., Loewen, P. C., and Fita, I. (1995) *Structure* **3,** 491–502
11. Bravo, J., Maté, M. J., Schneider, T., Switala, J., Wilson, K., Loewen, P. C., and Fita I. (1999) *Proteins* **34,** 155–166
12. Carpena, X., Soriano, M., Klotz, M. G., Duckworth, H. W., Donald, L. J., Melik-Adamyan, W., Fita, I., and Loewen, P. C. (2003) *Proteins* **50,** 423–436
13. Murshudov, G. N., Grebenko, A. I., Barynin, V., Dauter, Z., Wilson, K. S., Vainshtein, B. K., Melik-Adamyan, W., Bravo, J., Ferrán, J. M., Ferrer, J. C., Switala, J., Loewen, P. C., and Fita, I. (1996) *J. Biol. Chem.* **271,** 8863–8868
14. Bravo, J., Fita, I., Ferrer, J. C., Ens, W., Hillar, A., Switala, J., and Loewen, P. C. (1997) *Protein Sci* **6,** 1016–1023
15. Loewen, P. C., Switala, J., von Ossowski, I., Hillar, A., Christie, A., Tattrie, B., and Nicholls, P. (1993) *Biochemistry* **32,** 10159–10164
16. Nicholls, P., Fita, I., and Loewen, P. C. (2001) *Adv. Inorg. Chem.* **51,** 51–106
17. Melik-Adamyan, W., Bravo, J., Carpena, X., Switala, J., Maté, M. J., Fita, I., and Loewen, P. C. (2001) *Proteins* **44,** 270–281
18. Kalko, S. G., Gelpi, J. L., Fita, I., and Orozco, M. (2001) *J. Am. Chem. Soc.* **123,** 9665–9672
19. Amara, P., Andreoletti, P., Jouve, H. M., and Field, M. J. (2001) *Protein Sci.* **10,** 1927–1935
20. Sevinc, M. S., Mate, M. J., Switala, J., Fita, I., and Loewen, P. C. (1999) *Protein Sci.* **8,** 490–498
21. Mate, M. J., Sevinc, M. S., Hu, B., Bujons, J., Bravo, J., Switala, J., Ens, W., Loewen, P. C., and Fita, I. (1999) *J. Biol. Chem.* **274,** 27717–27725
22. von Ossowski, I., Mulvey, M. R., Leco, P. A., Borys, A., and Loewen, P. C. (1991) *J. Bacteriol.* **173,** 514–520
23. Mead, D. A., Skorupa, E. S., and Kemper, B. (1985) *Nucleic Acids Res.* **13,** 1103–1118
24. Yanisch-Perron, C., Vieria, C. J., and Messing, J. (1985) *Gene* (*Amst.*) **33,** 103–119
25. Kunkel, T. A., Roberts, J. D., and Zakour, R. A. (1987) *Methods Enzymol.* **154,** 367–382
26. Mulvey, M. R., Sorby, P. A., Triggs-Raine, B. L., and Loewen, P. C. (1988) *Gene* (*Amst.*) **73,** 337–345
27. Sanger, F. S., Nicklen, S., and Coulson, A. R. (1977) *Proc. Natl. Acad. Sci. U. S. A.* **74,** 5463–5467
28. Rorth, H. M., and Jensen, P. K. (1967) *Biochim. Biophys. Acta* **139,** 171–173
29. Ogura, Y. (1955) *Arch. Biochem. Biophys.* **57,** 288–300
30. Layne, E. (1957) *Methods Enzymol.* **3,** 447–454
31. Loewen, P. C., and Switala, J. (1986) *Biochem. Cell Biol.* **64,** 638–646
32. Otwinowski, Z., and Minor, W. (1996) *Methods Enzymol.* **276,** 307–326
33. Murshudov, G. N., Vagin, A. A., and Dodson, E. J. (1997) *Acta Crystallogr. Sect. D Biol. Crystallogr.* **53,** 240–255
34. Collaborative Computational Project, Number 4. (1994) *Acta Crystallogr. Sect. A* **50,** 760–763
35. Jones, T. A., Zou, J. Y., Cowan, S. W., and Kjeldgaard, M. (1991) *Acta Crystallogr. Sect. A* **47,** 110–119
36. Kleywegt, G. J., and Jones, T. A. (1994) *Acta Crystallogr. Sect. D Biol. Crystallogr.* **50,** 178–185
37. Evans, S. (1993) *J. Mol. Graphics.* **11,** 134–138
38. Schumb, W. C., Satterfield, C. N., and Wentworth, R. L. (1955) *Hydrogen Peroxide*, pp. 310–353, Reinhold, New York